Supplementary Information

Chirality-promoted photocatalysis: A Strategic Framework for Advancing Future Dye Degradation Technologies

Utpal Kumar Gosh, Anujit Balo, Koyel Banerjee Ghosh*

Department of Chemistry, Indian Institute of Technology Hyderabad, Telangana 502284, India

Corresponding Author

Koyel Banerjee Ghosh

Email: koyel@chy.iith.ac.in

Materials and chemicals

Rhodamine B (SRL), Methyl Orange (SRL), Chloroauric acid (HAuCl4, 99.9%, SRL), Cetyltrimethylammonium bromide (CTAB, 99%, SRL), Sodium borohydride (NaBH4, 99%, Sigma-Aldrich), D-Cysteine Hydrochloride monohydrate (99%, TCI), L-cysteine Hydrochloride hydrate (99%, Sigma-Aldrich), DL-cysteine Hydrochloride monohydrate (99%, TCI), L-Ascorbic acid (AA, 99%, TCI), 3-Mercaptopropionic acid (>98%, TCI) used in this work are of analytical grade and were used without further purification.

Synthesis of Chiral gold nanoparticles

The chiral gold nanoparticle was synthesized using the method described in the literature.[1] Initially, in a solution containing CTAB (100 mM, 7.5 mL) and $HAuCl_4$ (10 mM, 0.25 mL) was quickly mixed with a reducing agent, $NaBH_4$ (10 mM, 0.8 mL), and kept in 28 °C for 3 hours to allow full decomposition for creating a solution of tiny spherical seeds. Subsequently, the growth solution was prepared using the $1/10^{th}$ diluted seed solutions. In a typical synthesis process, $HAuCl_4$ (10 mM, 0.2 mL) was taken in an aqueous solution of CTAB (100 mM, 1.6 mL in 8 mL H_2O), followed by the addition of AA (50 mM, 0.95 mL). After that, the diluted seed solution was added and mixed rapidly. The solution turned pink after 15 minutes, signifying the formation of cuboctahedron nanoparticles. Then, the solution was centrifuged twice to remove the unreacted reactants and redispersed in a 1 mM CTAB solution. The chiral modification was carried out by taking previously synthesized nanoparticles (100 µL) in the mixture of CTAB (100 mM, 0.8 mL), $HAuCl_4$ (10 mM, 0.1 mL), AA (0.1 M, 0.475 mL) and cysteine (0.1 mM, 5 µL) in 3.95 mL H_2O. After rapid mixing, the solution was kept undisturbed for one hour at 30 °C bath. Finally, the solution was again centrifuged twice, redispersed in 0.1 mM CTAB solution, and used for further characterizations.

Characterizations

The crystalline properties of the as-prepared nanoparticles were analyzed via powder X-ray diffraction (XRD) technique in Empyrean (PAN analytical) powder X-ray diffractometer. Scanning electron microscopy (SEM, JEOL JIB-4700F) with an accelerating voltage of 15 kV and

transmission electron microscopy (TEM, JEOL JEM-2100FX) with an accelerating voltage of 200 kV were used to examine the catalyst's microstructure and morphology. UV–vis spectroscopy was recorded on a Jasco V-730 spectrophotometer, and CD spectroscopy measurements were performed using a JASCO-J815 CD spectrometer. The composition of the composite catalyst was revealed by using X-ray photoelectron spectroscopy (XPS). It was carried out using AXIS SUPRA system with a monochromatic Al X-ray source (photon energy 1486.69 eV). The internal structural analogy was examined by Fourier transform infrared (FTIR) techniques with JASCO FT/IR-4600 Fourier Transform Infrared spectrophotometer.

Calculation of g-factor

The g-factor value was calculated using the established formula reported in the previous literature.[2]

$$g = \frac{CD\ (mdeg)}{32980 \times Absorbance} \quad (1)$$

1. Optical analysis

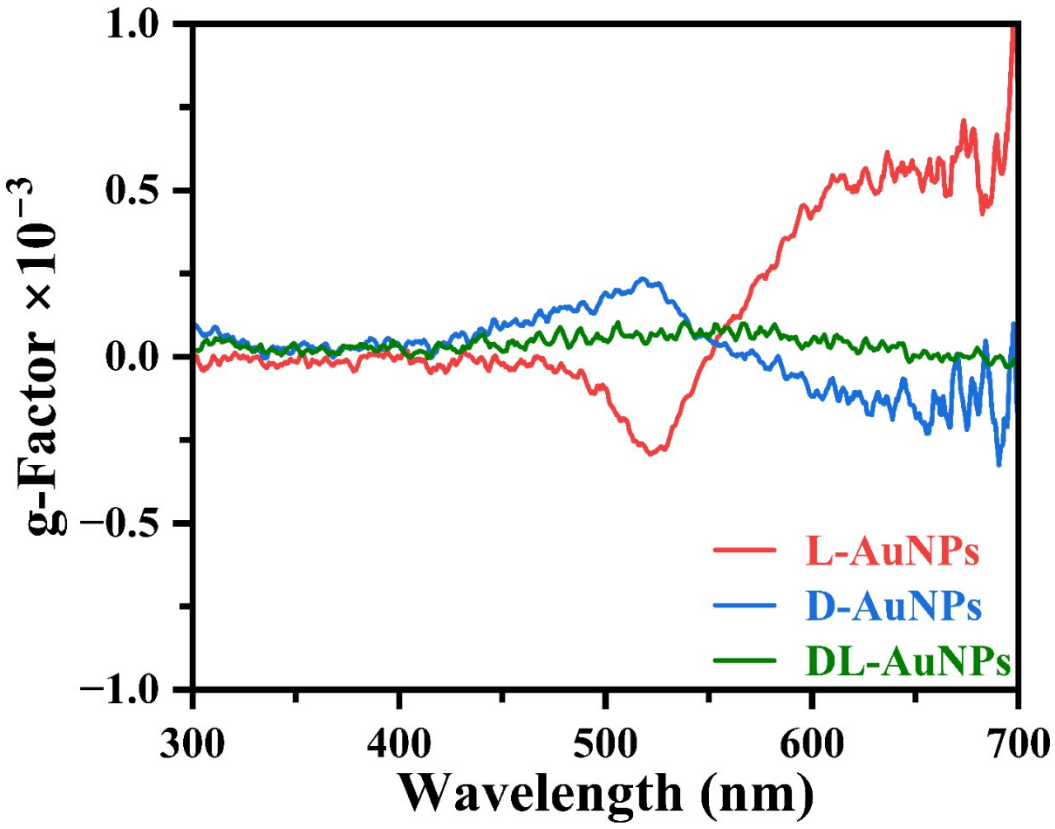

Figure S1. g-factor spectra of L-Au NPs (red), D- Au NPs (blue), and DL-Au NPs (green).

2. Morphology study

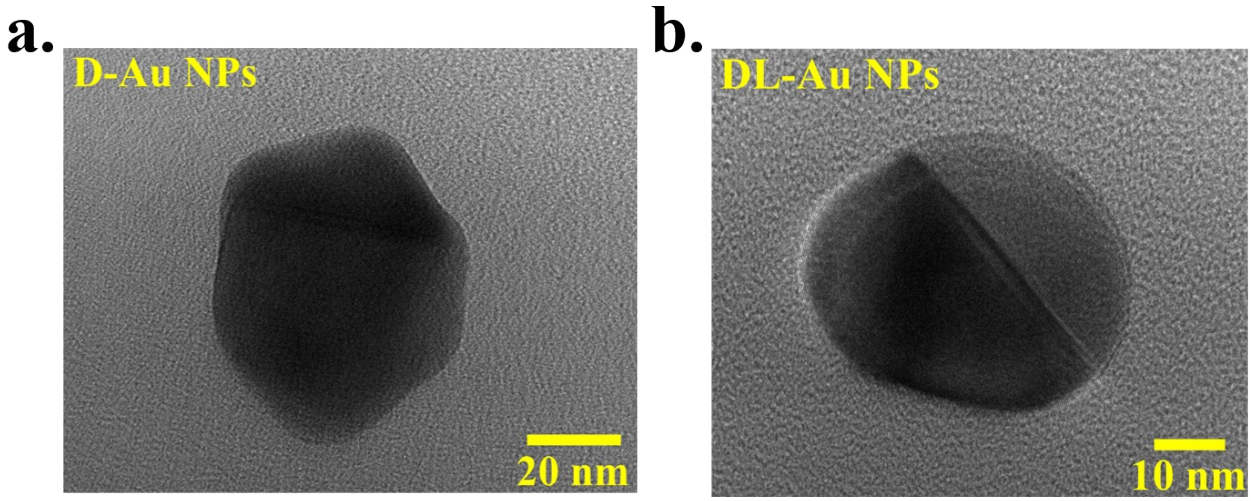

Figure S2. TEM image of a) D-Au NPs and b) L-Au NPs.

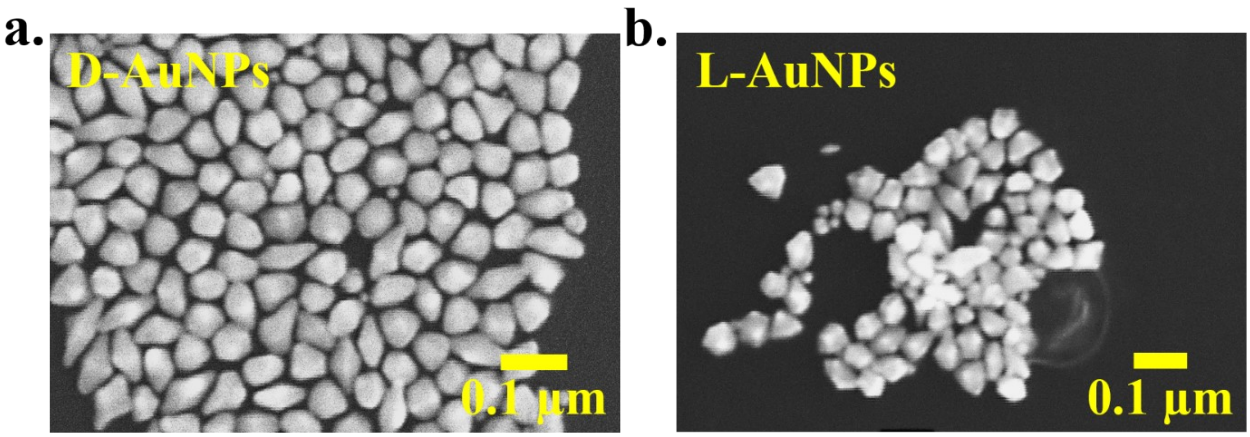

Figure S3. SEM image of a) D-Au NPs and b) L-Au NPs.

3. Photocatalytic study of Rhodamine B with different concentration

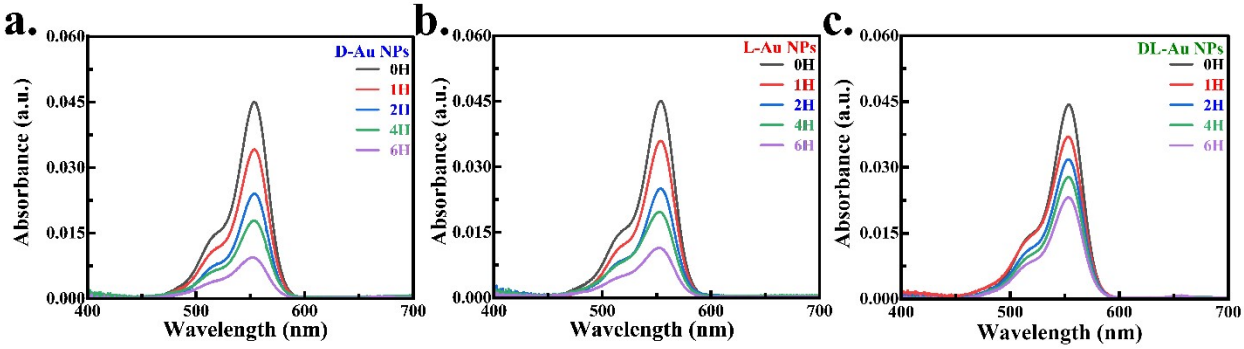

Figure S4. UV-Vis spectra of 0.5 µM RhB degradation by a. D-, b. L-, and c. DL-Au NPs at different time.

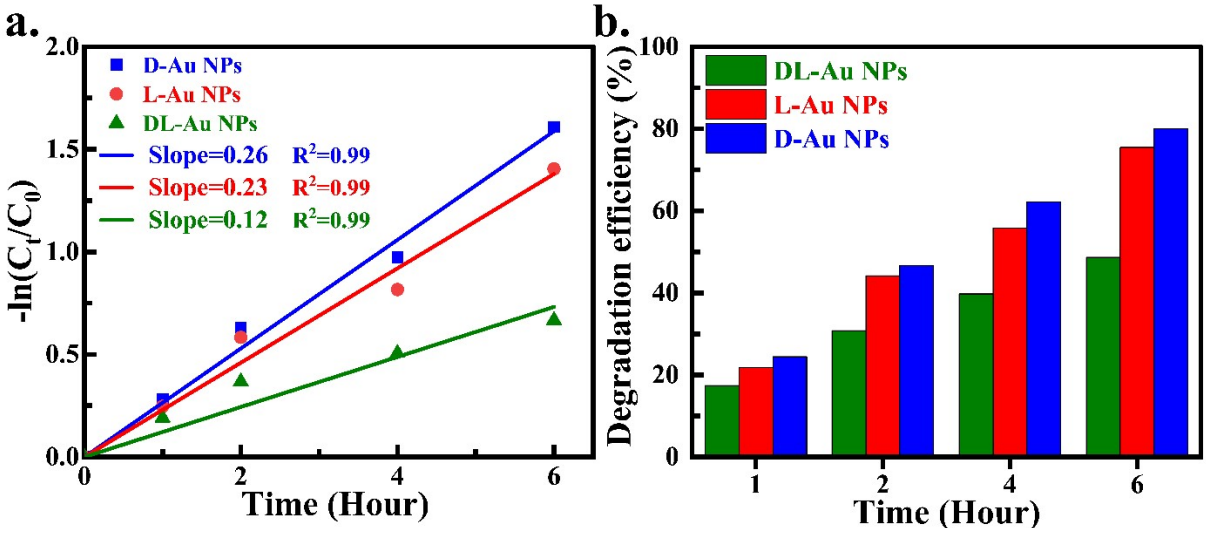

Figure S5. a. Kinetics $(-\ln(C_t/C_0)$ with respect to time (h)) plot of 0.5 μM RhB under visible light exposure. b. Comparison of 0.5 μM RhB degradation efficiency vs time for D-, L-, and DL-Au NPs photocatalyst.

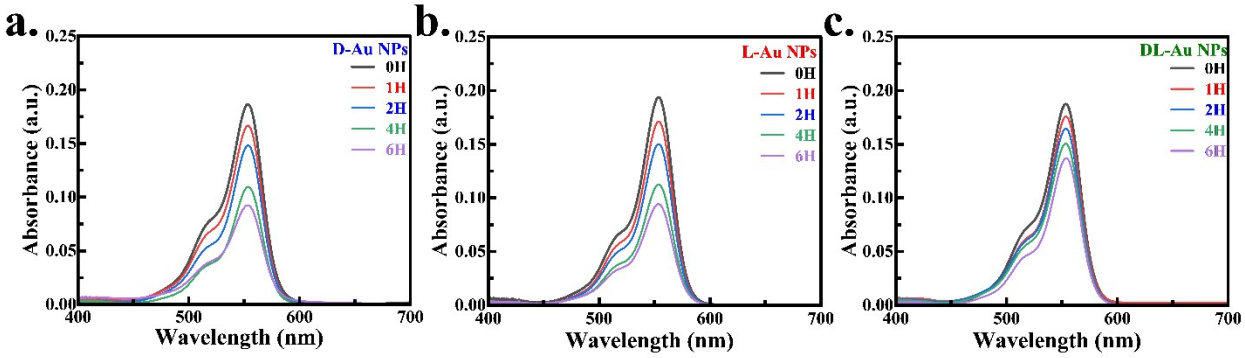

Figure S6. UV-Vis spectra of 2 μM RhB degradation by a. D-, b. L-, and c. DL-Au NPs at different time.

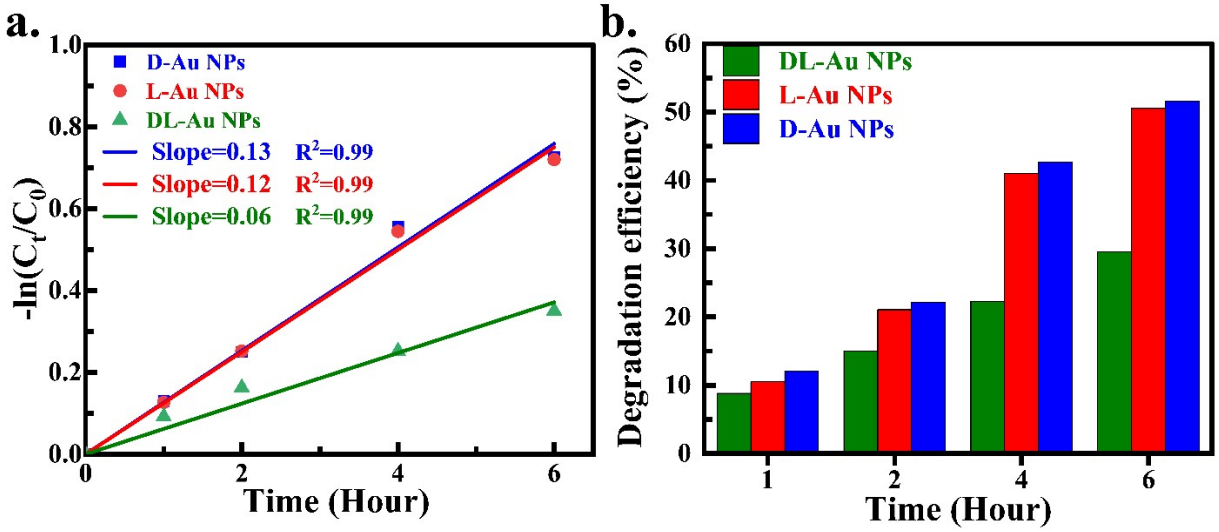

Figure S7. a. Kinetics $(-\ln(C_t/C_0)$ with respect to time (h)) plot of 2 μM RhB under visible light exposure. b. Comparison of 2 μM RhB degradation efficiency vs time for D-, L-, and DL-Au NPs photocatalyst.

4. Controlled experiment

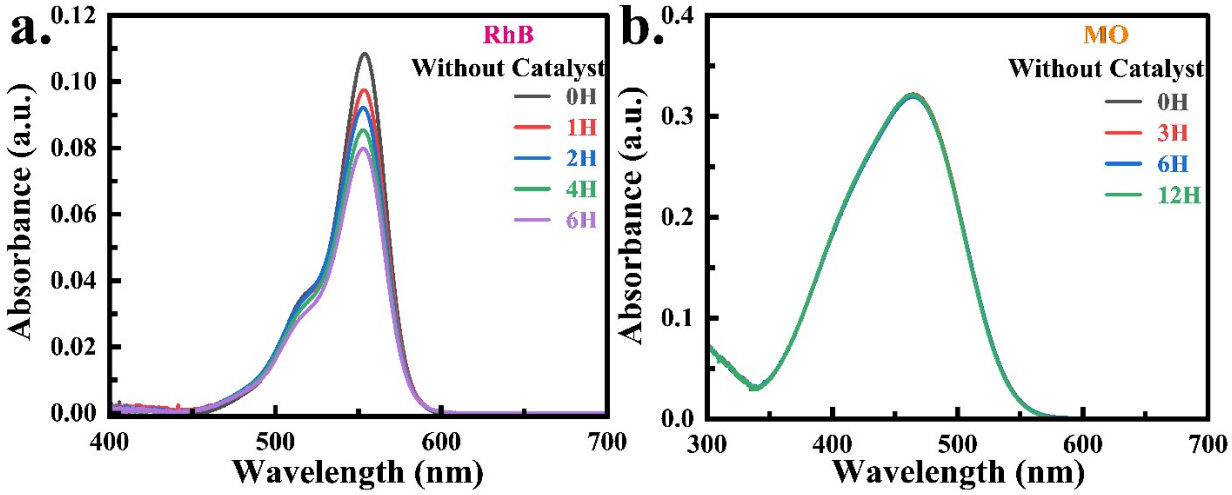

Figure S8. Photocatalysis of a) Rhodamine B and b) Methyl Orange in the absence of a catalyst at different irradiation time.

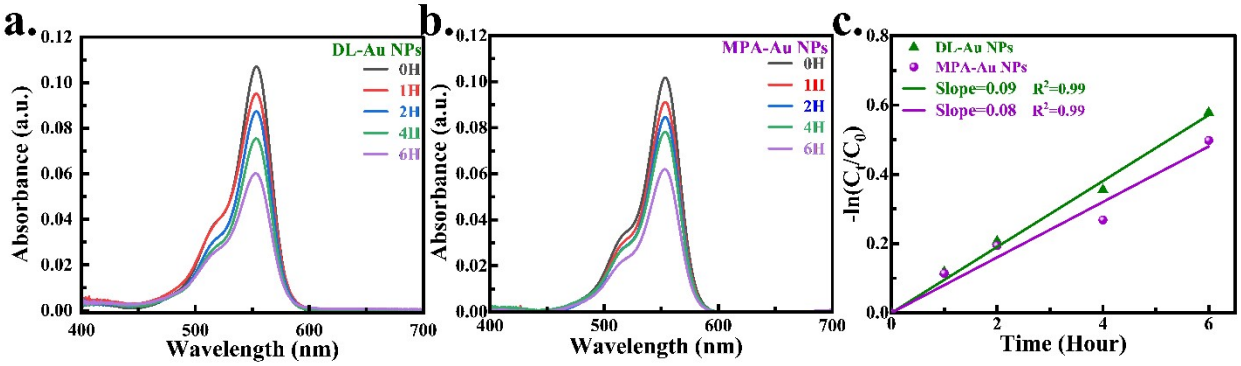

Figure S9. RhB degradation kinetics and Time-dependent photocatalytic activity study. (a) UV-Vis spectra of 1 µM RhB degradation by (a) DL-, (b) MPA-Au NPs at different time. (c) Kinetics ($-\ln(C_t/C_0)$ with respect to time (h)) plot of RhB under visible light exposure.

5. Post photocatalytic study

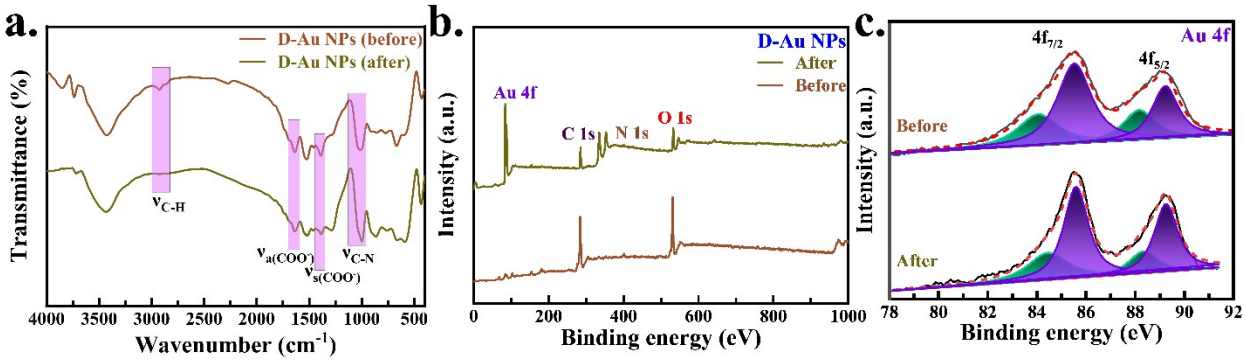

Figure S10. FTIR and XPS analysis. a. FTIR spectra, b. wide XPS spectra, and c. deconvoluted Au spectra of D-Au NPs before and after the catalysis.

6. Radical trapping experiments

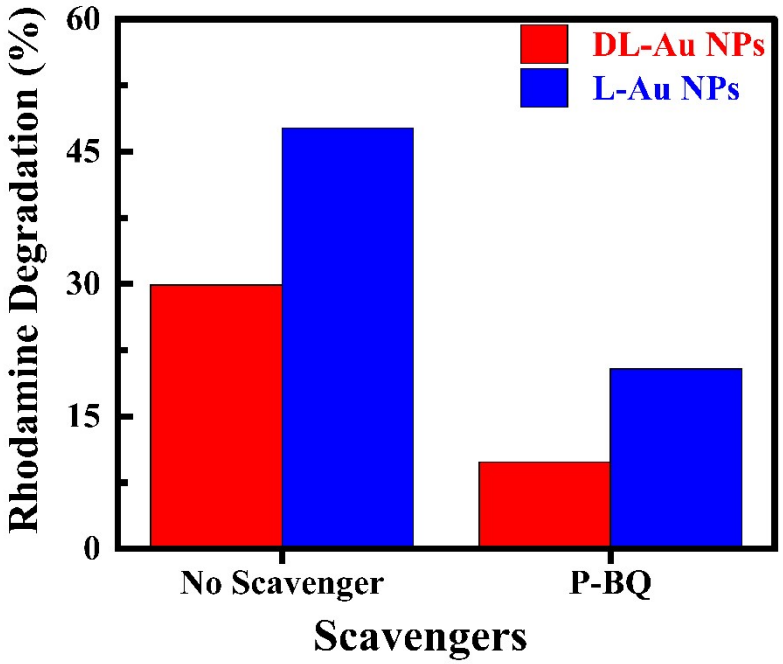

Figure S11. Light illumination time was 4h and 0.5 mM P-BQ was used for trapping the ROS.

7. Tables for error bars

Table S1: $-\ln(C_t/C_0$ vs time (h) plot's error bar values of three types of catalyst for 1µM RhB dye degradation.

Time (h)	D- Au NPs		L- Au NPs		DL- Au NPs	
	Mean	SE of mean	Mean	SE of mean	Mean	SE of mean
0	0	0	0	0	0	0
1	0.22	0.036	0.14	0.024	0.12	0.007
2	0.37	0.022	0.27	0.042	0.16	0.022
4	0.67	0.027	0.60	0.042	0.30	0.026
6	0.96	0.088	0.87	0.027	0.42	0.080

Table S2: Degradation efficiency (%) vs time (h) plot's error bar values of three types of catalyst for 1µM RhB dye degradation.

Time (h)	D- Au NPs		L- Au NPs		DL- Au NPs	
	Mean	SE of mean	Mean	SE of mean	Mean	SE of mean
0	0	0	0	0	0	0
1	19.33	2.921	13.03	2.109	10.86	0.588
2	30.81	1.499	23.53	3.221	14.97	1.883
4	48.90	1.402	44.73	2.388	26.15	1.878
6	61.28	3.287	58.16	1.140	34.06	5.059

Table S3: $-\ln(C_t/C_0)$ **vs time (h) plot's error bar values of three types of catalyst for 12µM MO dye degradation.**

Time (h)	D- Au NPs		L- Au NPs		DL- Au NPs	
	Mean	SE of mean	Mean	SE of mean	Mean	SE of mean
0	0	0	0	0	0	0
3	0.13	0.014	0.10	0.015	0.08	0.008
6	0.29	0.026	0.22	0.040	0.14	0.016
12	0.46	0.036	0.41	0.019	0.30	0.015

Table S4: Degradation efficiency (%) vs time (h) plot's error bar values of three types of catalyst for 12µM MO dye degradation.

Time (h)	D- Au NPs		L- Au NPs		DL- Au NPs	
	Mean	SE of mean	Mean	SE of mean	Mean	SE of mean
0	0	0	0	0	0	0
3	12.21	1.224	9.69	1.306	7.30	0.702
6	24.77	1.932	22.01	1.262	12.79	1.416
12	37.05	2.225	33.40	1.279	25.53	1.143

References:

1 H.-E. Lee, R. M. Kim, H.-Y. Ahn, Y. Y. Lee, G. H. Byun, S. W. Im, J. Mun, J. Rho and K. T. Nam, *Nat. Commun.*, 2020, **11**, 263.

2 M. Mandal, A. Yadav, M. Malik, S. Das, A. Mahapatra, K. P. Katin and P. C. Mondal, *Adv. Funct. Mater.*, 2025, **n/a**, e17488.